confirmed this diagnosis by immunohistochemistry to demonstrate absence of LAMP-2 in skeletal muscle. Age at muscle biopsy varied from one year to 29 years, average 15 years ± 9. One patient underwent 2 biopsies from his left biceps brachii muscle at ages one year and from his right quadriceps femoris muscle at age 16 years (12). We also studied muscle from a 2-month-old boy with infantile AVM (7), a 41-year-old man with adult-onset AVM with multiorgan involvement (8), and an 18-year-old man with probable XMEA who showed typical clinicopathologic features of the disease but without a family history of myopathy.

Control specimens were obtained from 10 individuals with morphologically normal muscle. In addition, we also studied muscle from 21 patients with AMD (9 infants, 6 children, and 6 adults), 18 patients with DMRV/HIBM, and 20 patients with SIBM. We confirmed that all DMRV/HIBM patients had mutations in the gene encoding UDP-N-acetylglucosamine 2-epimerase/N-acetylmannosamine kinase (13).

Histochemistry

All biopsy specimens were taken from either the biceps brachii or quadriceps femoris muscle. These tissue samples were frozen in liquid nitrogen-cooled isopentane for histochemistry and immunohistochemistry. Transverse serial frozen sections of 8-μm thickness were stained with hematoxylin and eosin (H&E), modified Gomori trichrome, and a battery of histochemical methods, including AChE and NSE stains.

Immunohistochemistry

We performed indirect immunofluorescence staining on 5-μm serial cryosections of muscle according to previously described methods (14). These sections were incubated at 37°C for 2 hours with primary mouse monoclonal IgG antibodies against AChE, lysosomal membranous proteins: LAMP-1, lysosomal integral membrane protein-1 (LIMP-1), LIMP-2, and 19 primary monoclonal or polyclonal antibodies against various sarcolemmal proteins and extracellular matrix proteins (Tables 1 and 2). We also used antibodies against an intralysosomal protein, cathepsin L, and endosomal proteins, VAMP-7, Rab5, transferrin receptor (TfR), and low-density lipoprotein receptor (LDL-R). These were subsequently incubated at room temperature for 1 hour with a secondary antibody, fluorescein isothiocyanate (FITC)-labeled goat F(ab')2 anti-mouse IgG (Leinco Technology, St. Louis, MO) or anti-rabbit IgG (H&L) (Leinco). For double immunolabeling using mouse monoclonal anti-LIMP-1 and rabbit polyclonal anti-dystrophin antibodies (a generous gift from Dr. Imamura), we used two secondary antibodies: FITC-labeled anti-mouse IgG (Leinco) and rhodamine-labeled anti-rabbit IgG (Leinco). We also have stained serial sections with Alexa 488 conjugated α-bungarotoxin (Molecular Probe, Eugene, OR) and were examined by fluorescence microscopy. Furthermore, in other sections, after incubation with primary antibodies we stained with the avidin-biotin-peroxidase complex method (Vector Laboratories, Burlingame, CA) using another secondary antibody: biotinylated goat anti-mouse IgG (Vector). The reaction was visualized with 3,3′-diaminobenzidine (DAB) as the substrate, yielding a brown reaction product. Normal mouse IgG, diluted to the same concentration as the primary antibodies, was used as a negative control.

To estimate presence of the sarcolemmal proteins in vacuolar membrane, we scored the signal of the antibodies from negative (−) to strong (+++) relative to their immunoreactivity in the sarcolemma. The strong score (+++) indicates that the reactivity level in vacuoles equals that in the sarcolemma. Moreover, we counted the numbers of 1) muscle fibers with intracytoplasmic vacuoles highlighted with dystrophin, and 2) muscle fibers with intracytoplasmic overexpression of LIMP-1, in randomly selected fields of all the patients, and calculated the average percentages of both types of muscle fibers in each patient. Statistical analysis of the correlation between the age of the patients and the numbers of muscle fibers immunoreacting dystrophin or LIMP-1 was performed using linear regression.

Electron Microscopy

For electron microscopy, biopsy specimens were fixed in buffered 2% isotonic glutaraldehyde at pH 7.4, postfixed in osmium tetroxide, and embedded in Epoxy resin. Ultrathin sections were stained with uranyl acetate and lead nitrate, and examined with an H-7000 electron microscope (Hitachi, Tokyo, Japan).

Immunoelectron Microscopy

We performed immunoelectron microscopy by preembedding labeling methods. We used muscle biopsy specimens frozen in liquid nitrogen-cooled isopentane without paraformaldehyde prefixation. The specimens were cut in a cryostat into 10-μm transverse sections without thawing and fixed in chilled 4% paraformaldehyde solution in 0.1M phosphate buffer (pH 7.4) for 10 minutes. The fixed sections were washed 5 times in phosphate-buffered saline (PBS). To eliminate nonspecific reactions, sections were incubated for 30 minutes at room temperature in PBS containing 10% normal goat serum and 1% bovine serum albumin (BSA) with PBS. The sections were then incubated at 4°C overnight with one of the following primary mouse monoclonal IgG antibodies: LIMP-1 and the C-terminus of dystrophin. After washing for 30 minutes in PBS, the sections were incubated at 4°C overnight with a secondary antibody: 10-nm-gold-labeled rat anti-mouse antibody (British Biocell International, Cardiff, UK). Subsequently, the sections were fixed in 0.5% glutaraldehyde and postfixed in osmium, and embedded in Epoxy resin. Ultrathin sections were counterstained with uranyl acetate and lead nitrate.

LAMP-2-Deficient Mice and Pathological Methods

We analyzed tibialis anterior muscle from 2 LAMP-2-deficient mice (10, 11) at ages 4 months and 16 months and age-matched normal mice. Muscle specimens were frozen in liquid nitrogen-cooled isopentane for histochemistry and immunohistochemistry or fixed with glutaraldehyde for electron microscopy. Transverse serial frozen sections of 10-μm thickness were stained with H&E, modified Gomori trichrome,

TABLE 1. Summary of Histochemistry and Immunohistochemistry in Various Myopathies with Autophagic Vacuoles

			Expression on Vacuolar Membrane		
	Manufacturer of Antibody	Dilution	Danon Disease and Related AVMs	Rimmed Vacuolar Myopathies	AMD
Histochemistry					
NSE	–	–	+++	–	–
AChE	–	–	+++	–	–
PAS	–	–	+	–	+++
Acid P	–	–	± to ++	++	++
Immunohistochemistry					
AChE	Chemicon, Temecula, CA	1:2000	+++	–	–
AChR	Molecular Probe, Eugene, OR	1:300	–	–	–
C-terminus of Dystrophin	Novocastra, Newcastle Upon Tyne, UK	1:100	+++	– to +	– to +
Rod domain of Dystrophin	Novocastra	1:50	+++	– to +	– to +
N-terminus of Dystrophin	Novocastra	1:20	+++	– to +	– to +
α-Sarcoglycan	Novocastra	1:100	+++	– to +	– to +
β-Sarcoglycan	Novocastra	1:100	+++	– to +	– to +
γ-Sarcoglycan	Novocastra	1:200	++	– to +	– to +
δ-Sarcoglycan	Novocastra	1:50	+++	– to +	– to +
α-Dystroglycan	Upstate, Lake Placid, NY	1:100	++	– to +	– to +
β-Dystroglycan	Novocastra	1:200	+++	– to +	– to +
Dystrobrevin	RDI, Flanders, NJ	1:100	++	– to +	– to +
Dysferlin	Novocastra	1:50	++	– to +	– to ±
Utrophin	Novocastra	1:50	+	– to ±	–
Caveolin-3	Transduction Labs, Lexington, KY	1:100	++	– to +	– to +
β-Spectrin	Novocastra	1:100	++	– to +	– to +
Laminin α2	Chemicon,	1:5000	++	– to +	– to +
Integrin β1	Genex, Helsinki, Finland	1:100	+++	– to +	– to +
Perlecan	Chemicon	1:100	++	– to +	– to +
Agrin	A generous gift from Dr. Sugiyama (32)	1:100	++	– to +	– to +
Fibronectin	Biomedical Tech., Stoughton, MA	1:1000	++	– to ±	– to ±
Collagen IV	Novocastra	1:1000	– to +	– to ±	– to ±
Collagen VI	ICN, Aurora, OH	1:500	– to +	–	– to ±

Both antibodies against fibronectin and agrin were rabbit polyclonal antibodies. All the other antibodies were mouse monoclonal antibodies. AChR was evaluated by binding to α-bungarotoxin. AMD, acid maltase deficiency; NSE, non-specific esterase; AChE, acetylcholinesterase; PAS, periodic acid Schiff; Acid P, acid phosphatase; AchR, acetylcholine receptor.

and a battery of histochemical methods, and the same immunohistochemical methods described above.

RESULTS

Histochemistry and Immunohistochemistry

By routine histologic studies, the vacuolar membranes in Danon disease, probable XMEA, infantile AVM and adult-onset AVM were essentially identical (Table 1). All muscle samples showed mild to moderate variation in fiber size. There were no necrotic fibers except in muscle from adult-onset AVM, which revealed a few necrotic and regenerating fibers. There were scattered small basophilic granules rather than vacuoles in the muscle fibers in H&E-stained sections (Fig. 1). Histochemistry revealed AChE and NSE activities in the vacuolar membranes and the vacuolar structures of the granules. Immunohistochemistry also confirmed presence of AChE in those vacuoles. However, they did not bind to α-bungarotoxin, indicating the absence of acetylcholine receptors (AChRs) in the vacuolar membranes.

By immunohistochemistry, the AVSF reacted for all the tested sarcolemmal and extracellular matrix proteins in the vacuolar membranes in muscle from patients with Danon disease and related AVMs, although reactivity levels of the proteins were variable (Table 1; Fig. 1). However, only collagens IV and VI showed less intense reactivity in the vacuolar membranes than that in the sarcolemma. Most of the AVSFs were scattered throughout the cytoplasm rather than clustered in the subsarcolemmal region. On serial transverse 5-μm sections, most of the AVSFs formed a closed space and the vacuolar membranes were not connected to the sarcolemma with only a few exceptions (Fig. 1Y). Longitudinal sections demonstrated the oval shape of the AVSF, confirming the closed structure of the vacuoles (Fig. 1Z). Vacuolar membranes connected to the sarcolemma were seen in only 2 patients; both were more than 20 years old.

In muscle from patients with Danon disease, LIMP-1, a lysosomal membrane protein, showed accumulations scattered

TABLE 2. Summary of Lysosomal and Endosomal Proteins for Immunohistochemistry in Danon Disease and Related AVMs

Antigen	Manufacturer	Dilution	Expression in the Muscle Fibers
Lysosomal protein			
LAMP-1	Developmental Studies Hybridoma Bank (DSHB), Iowa City, IA	1:100	++
LAMP-2	DSHB	1:100	−
LIMP-1	DSHB	1:100	+++
LIMP-2	A generous gift from Dr. Tanaka (10)	1:200	+
Cathepsin L	Abcam, Cambridge, UK	1:100	+
Endosomal protein			
Rab5	BD Bioscience, Franklin Lakes, NJ	1:50	+
LDL-R	Progen Biotechnik, Heidelberg, Germany	1:100	+
VAMP-7	A generous gift from Dr. Galli (29)	1:200	++
Transferrin R	Lab Vision, Fremont, CA	1:100	+

Antibody against LIMP-2 was rabbit polyclonal and antibody against LDL-R was chicken polyclonal. All the other antibodies were mouse monoclonal.

throughout the fibers in a distribution identical to that of the small basophilic granules on H&E-stained sections (Fig. 2; Table 2), indicating that most autophagic vacuoles in Danon disease are autolysosomes. These autolysosomal accumulations were surrounded by dystrophin-positive membranes in some fibers but not in others (Fig. 2). LAMP-1 and LIMP-2 showed slightly increased expression in fibers with LIMP-1-positive granules (data not shown). Muscle fibers with dystrophin-positive vacuoles accounted for 0.5% to 14.3%, increasing in proportion with age ($y = 0.016 + 0.40x$, $r = 0.94$; Fig. 3). Muscle fibers with autolysosomal accumulations, both with and without dystrophin-positive vacuolar membranes, accounted for 23.7% to 28.7%, showing a slight tendency to decrease with age ($y = 28.6 - 0.15x$, $r = 0.71$; Fig. 3).

LDL-R, TfR, and Rab5 showed mild upregulation mainly in fibers with autolysosomal accumulations in Danon disease and related AVMs (Table 2). Cathepsin L was expressed weakly, mainly in fibers with autolysosomal accumulations. Only VAMP-7 was strongly expressed, mainly in the non-vacuolated fibers without autolysosomal accumulations.

There were occasional intracytoplasmic vacuoles with sarcolemmal proteins in muscles from patients with other AVMs (i.e. DMRV/HIBM, SIBM, and AMD) but their presence was less consistent than in Danon disease and related AVMs. In addition, they never showed AChE or NSE activity. In DMRV/HIBM and SIBM, fibers with sarcolemmal protein-associated vacuoles accounted for approximately 5% to 15% of fibers with rimmed vacuoles (Fig. 4; Table 1). In AMD, sarcolemmal and extracellular matrix proteins were present in some vacuolar membranes. The frequency of fibers with sarcolemmal proteins-associated vacuoles was less than 5% of vacuolated fibers in infantile AMD, and 10% to 15% of vacuolated fibers in childhood and adult-onset AMD.

Electron Microscopy and Immunoelectron Microscopy

In Danon disease and related AVMs, electron microscopy revealed scattered clusters of autophagic vacuoles containing cytoplasmic debris, electron dense materials, and myeloid bodies. Some of these autophagic vacuoles had basal lamina on the luminal side, while other clusters were not limited by a membrane (Fig. 5).

Immunoelectron microscopy showed many autophagic vacuoles; however technical limitations posed by preparing samples from frozen tissue without prefixation prevented us from clearly defining vacuolar membranes. At higher magnification, dystrophin signals were detected on the cytoplasmic side of the vacuolar membrane and along the periphery of the vacuoles (Fig. 5). In contrast, the LIMP-1 antibody signals were associated with autophagic materials including glycogen particles and cytoplasmic debris within the vacuoles, suggesting that the vacuoles are limited by membranes with sarcolemmal features and contain multiple small autophagic vacuoles derived from autolysosomes.

Muscle Pathology in Mice

Muscles from LAMP-2-deficient mice at both 4 and 18 months of age showed features of AVSFs at both light and electron microscopic levels. There were slight variations in fiber size and small vacuoles with basophilic granules by H&E. The granules contained acid phosphatase-positive material. These AVSFs had AChE and NSE activities similarly to those in Danon disease. The frequency of muscle fibers with the AVSFs decorated by NSE and AChE activities was 0.4% at 4 months and 8% at 16 months (data not shown). On immunohistochemistry, the vacuolar membranes were stained with antibodies against dystrophin and other sarcolemmal proteins as well as extracellular matrix proteins, whereas LAMP-2 was completely absent in the muscle. On electron microscopy, there were scattered intracytoplasmic autophagic vacuoles with glycogen particles and cytoplasmic debris (data not shown).

DISCUSSION

In muscle from patients with Danon disease and related AVMs, the membranes of AVSF showed immunoreactivity for all of the sarcolemmal and extracellular matrix proteins tested. Dystrophin and dystrobrevin are cytoskeletal proteins localized along the cytoplasmic side of the sarcolemma (15). Sarcoglycans and β-dystroglycan are transmembranous proteins and are components of "dystrophin bolts" (16). Utrophin

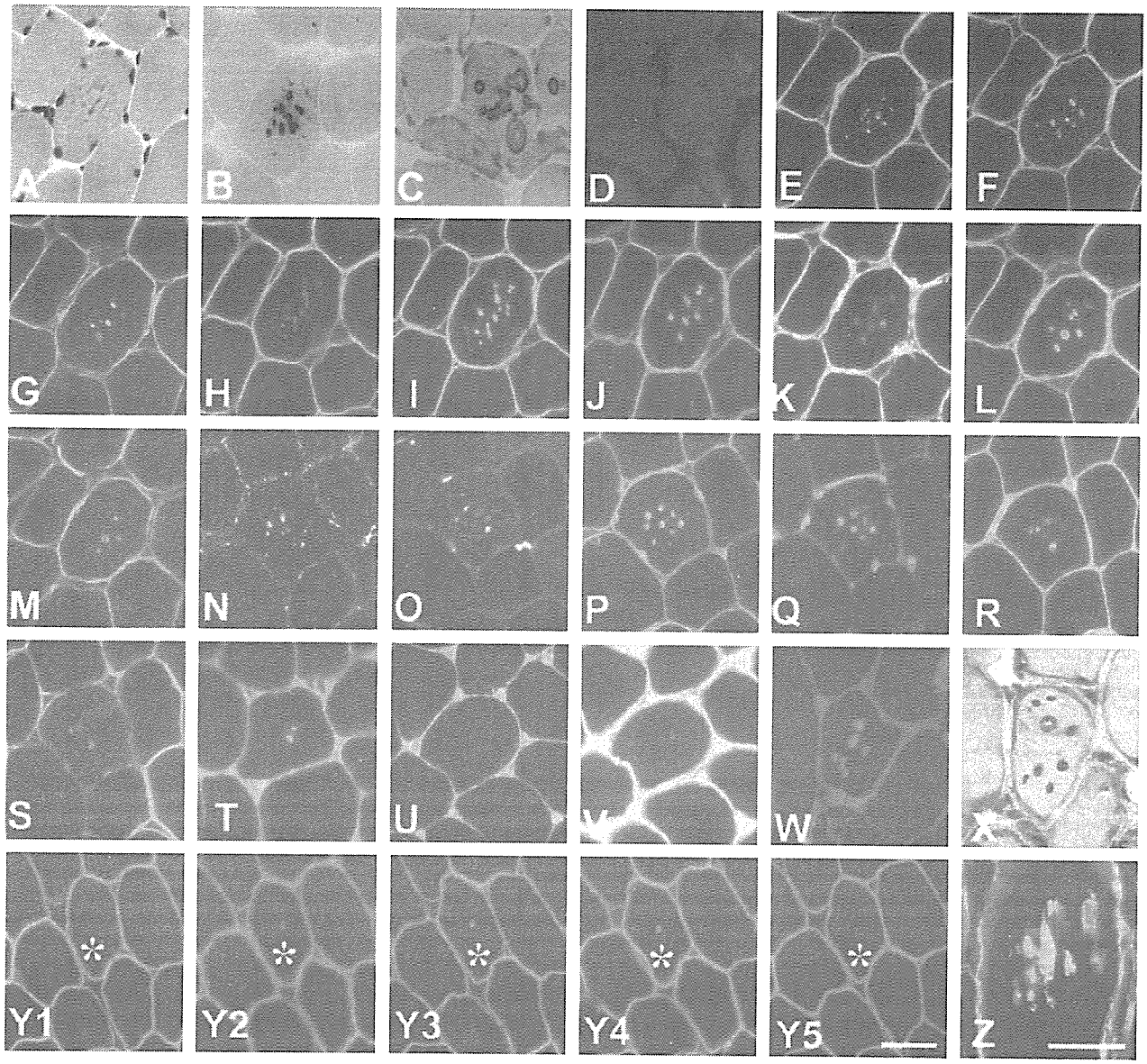

FIGURE 1. Histochemistry and immunohistochemistry. Transverse sections of skeletal muscle biopsies from Danon disease patients. Several fibers contain scattered tiny basophilic intracytoplasmic vacuoles **(A)**: H&E. The vacuolar membrane has high nonspecific esterase **(B)** and acetylcholinesterase **(C)** activities. None of the vacuoles bind to α-bungarotoxin **(D)**. Sections were stained with antibody against the C-terminus of dystrophin **(E)**, the rod domain of dystrophin **(F)**, the N-terminus of dystrophin **(G)**, laminin α2 **(H)**, α-sarcoglycan **(I)**, β-sarcoglycan **(J)**, γ-sarcoglycan **(K)**, δ-sarcoglycan **(L)**, dystrobrevin **(M)**, α-dystroglycan **(N)**, utrophin **(O)**, dysferlin **(P)**, β-dystroglycan **(Q)**, perlecan **(R)**, caveolin-3 **(S)**, collagen IV **(T)**, fibronectin **(U)**, collagen VI **(V)**, integrin β1 **(W)**, and agrin **(X)**. The vacuolar membranes were immuno-positive with most of the primary antibodies, although reactivity of these proteins was variable. The results are summarized in Table 1. Transverse 5-μm serial sections **(Y1–Y5)** and longitudinal section **(Z)** of muscle from Danon disease patient showing immunoreaction for dystrophin. Vacuolar membrane in muscle fiber (*) is not connected to the sarcolemma but is closed. Longitudinal section shows that the vacuoles are spherical or oval. **(D–W, Y1–Y5, Z)**: FITC-labeled staining; **(X)**: DAB staining. **(C–S, U, V, Y1–Y5)**: serial sections. Scale bars: **(A–W, Y1–Y5)** = 20 μm; **(Z)** = 30 μm.

is a submembranous protein structurally similar to dystrophin and is widely expressed, albeit at low levels, in the sarcolemma (17). Integrin β1 and α7 are transmembranous proteins and form a complex with each other in the sarcolemma (18). Dysferlin and caveolin-3 are also sarcolemmal proteins and are responsible for limb-girdle muscular dystrophy (LGMD) 2B and LGMD 1C, respectively (19, 20). Extracellular proteins, collagen IV, perlecan, fibronectin, agrin, and laminin, are the

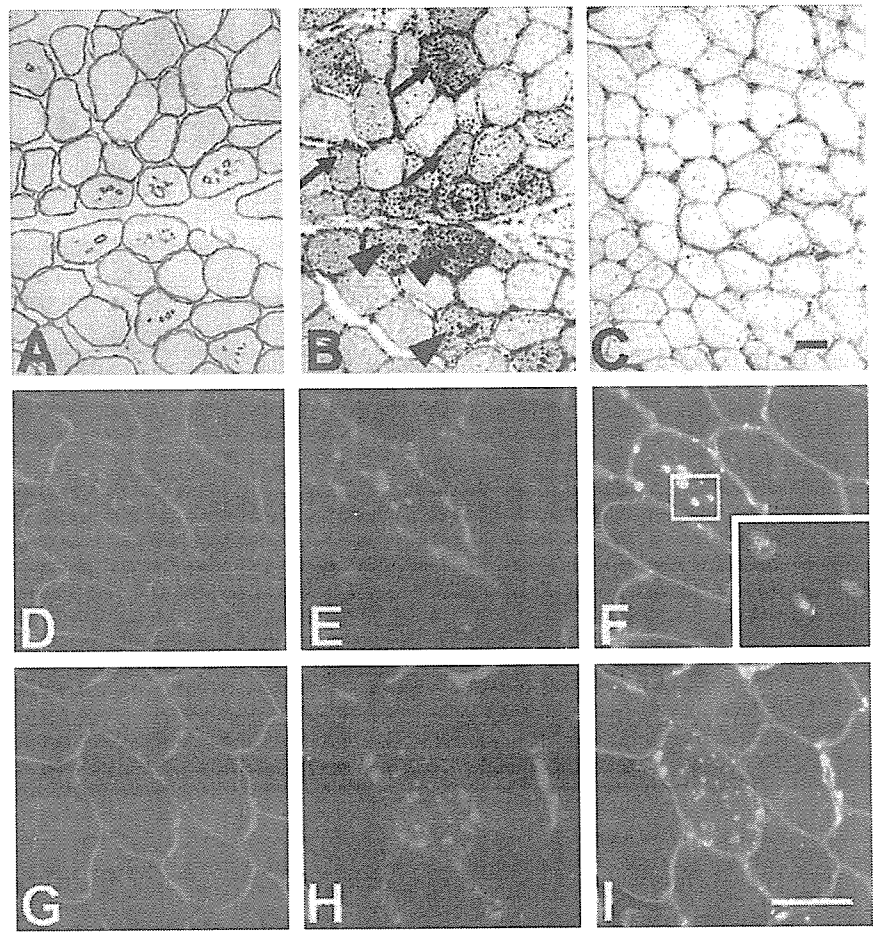

FIGURE 2. Indirect immunohistochemistry. Transverse sections of skeletal muscle stained with DAB for dystrophin (A) and LIMP-1 (B, C). (A, B) Danon disease patient; (C): Normal control. In Danon disease some muscle fibers express both LIMP-1 and dystrophin (arrowheads), whereas some muscle fibers show overexpression of LIMP-1 with absence of dystrophin (arrows). Normal control showed almost no expression of LIMP-1 (C) in muscle fibers. Scale bar = 40 μm. Double immunohistochemistry. Transverse sections of skeletal muscle from Danon disease patient, stained for dystrophin and LIMP-1. LIMP-1 is strongly accumulated inside the muscle fibers (D, G). In some muscle fibers, LIMP-1-positive accumulations are clearly surrounded by dystrophin immunopositive membrane (D–F). These vacuoles are the AVSF. In other muscle fibers, LIMP-1-positive accumulations are not surrounded by dystrophin (G–I). (D, G): dystrophin; (E, H): LIMP-1; (F, I): merged. Scale bar = 30 μm.

main components of the basal lamina. Collagen VI is present in the interstitium but is associated directly with collagen IV (21). We observed very little staining of only collagens IV and VI in vacuolar membranes, indicating that the membranes hardly contain these collagens. Based on our findings, we deduce that the vacuolar membrane of AVSFs in Danon disease and related AVMs have most of the sarcolemmal proteins ranging from cytoplasmic dystrophin to the extracellular laminin.

The vacuolar membranes of AVSF have abundant activities of AChE similar to neuromuscular junctions. Nevertheless, they are distinct from motor endplates because the membranes lacked AChRs. In the early stages of formation of the neuromuscular junction, AChE and AChRs are localized diffusely throughout the sarcolemma. When axon terminals make contact with muscle cells, postjunctional folds are quickly formed. In this process, AChE and AChRs accumulate at junctions and disappear from the extra-junctional sarcolemma (22, 23). These facts support our hypothesis that the vacuoles are intracellular enclosed spaces, because, if AVSF were derived from sarcolemma, then AChE-expressing vacuoles should be located near neuromuscular junctions rather than scattered in the cytoplasm. Furthermore, the presence of AChE without AChRs clearly indicates that the vacuolar membranes are distinct from either junctional or extra-junctional sarcolemma and suggests that they are formed through a unique process.

In the intracellular degradative process called autophagy, "isolation membranes" initially sequesters portions of cytoplasm to be degraded and forms "autophagosomes," which then fuse with lysosomes and become "autolysosomes." The cytoplasm sequestered in autolysosomes is then digested by proteolytic enzymes provided by the lysosomes. Most autophagic vacuoles in Danon disease are autolysosomes rather than autophagosomes, which lack enzymatic activity. These are indicated by the demonstration of many LIMP-1-positive accumulations scattered throughout the fibers (24, 25) and the autophagic nature of the vacuoles on electron microscopy. Actually, small basophilic granules on hematoxylin and eosin are most likely these autolysosomal accumulations as suggested by their pattern of distribution and the fact that lysosomes are basophilic on H&E. Moreover, some clusters of autolysosomes are surrounded by membranes with sarcolemmal features but others are not. In support of this notion, ultrastructural studies identified 2 types of autophagic vacuoles: 1) clusters of autophagic vacuoles not surrounded by membranes or basal lamina, and 2) vacuoles containing various

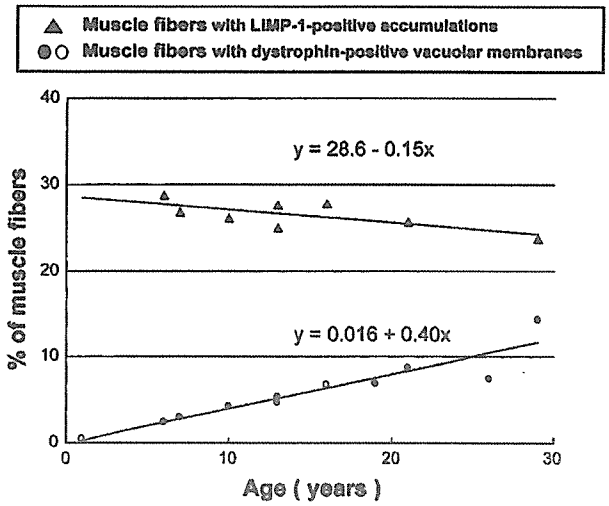

FIGURE 3. Relationship between age of the patients with Danon disease and number of muscle fibers with vacuoles highlighted with dystrophin or LIMP-1 on immunohistochemistry. The open circles show the only patient who had 2 muscle biopsies. The muscle fibers (circles) with intracytoplasmic vacuoles surrounded by dystrophin immuno-positive membrane (AVSFs) increased with age ($r = 0.936$). The muscle fibers (triangles) with overexpression of LIMP-1 showed a slight decrease with age ($r = 0.353$). r, Pearson's linear correlation coefficient.

autophagic materials encircled by membranes with basal lamina along the luminal side.

The proportion of muscle fibers with AVSFs increased with age in Danon disease and LAMP-2-deficient mice. In contrast, muscle fibers with LIMP-1-positive autolysosomal accumulations existed even in young patients and decreased slightly with age. It is most likely that the formation of these autolysosomal accumulations, which are clusters of autophagic vacuoles seen on electron microscopy, is a primary change in muscle fibers of Danon disease and related AVMs. The formation of peculiar membranes with sarcolemmal features around the autophagic vacuoles is hence a secondary phenomenon. Since muscle symptoms progress slowly in Danon disease, the development of muscle symptoms might be associated more closely with the formation of the unusual autophagic vacuoles rather than directly with the deficiency of LAMP-2.

LAMP-1 is the autosomal paralogous counterpart of LAMP-2 and both are thought to protect lysosomal membrane and cytoplasm from proteolytic enzymes within the lysosomes. LAMP-2 is tissue-specific but unlike LAMP 1, which is ubiquitously expressed, its expression is likely to be specifically regulated (26). Inhibition of LAMP-1 function results in failure of fusion of lysosomal and plasma membranes and therefore impaired exocytosis (27), a process usually by which cytoplasmic debris in the autophagosomes are extruded out from the cell through the sarcolemma (28). We therefore assume that LAMP-2 deficiency might likewise be related to dysregulation of exocytosis, leading to the development of the

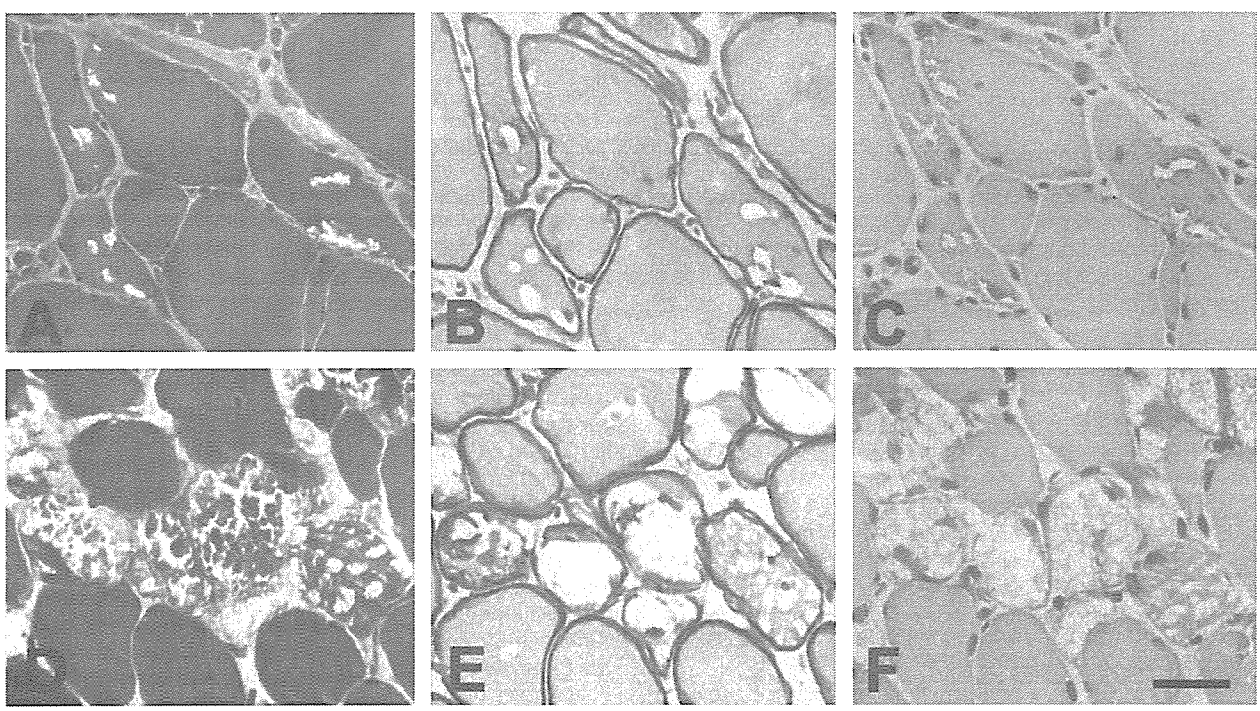

FIGURE 4. Transverse serial sections of muscle of patient with DMRV/HIBM (A–C) and with childhood AMD (D–F). Only a few rimmed vacuoles in DMRV/HIBM showed presence of dystrophin. In AMD, dystrophin is present on some vacuolar materials. However, no vacuolar membranes have AChE activity in DMRV/HIBM and AMD. (A, D): Gomori-trichrome stain; (B, E): AChE stain; (C, F): immunohistochemistry against dystrophin with DAB. Scale bar = 30 μm.

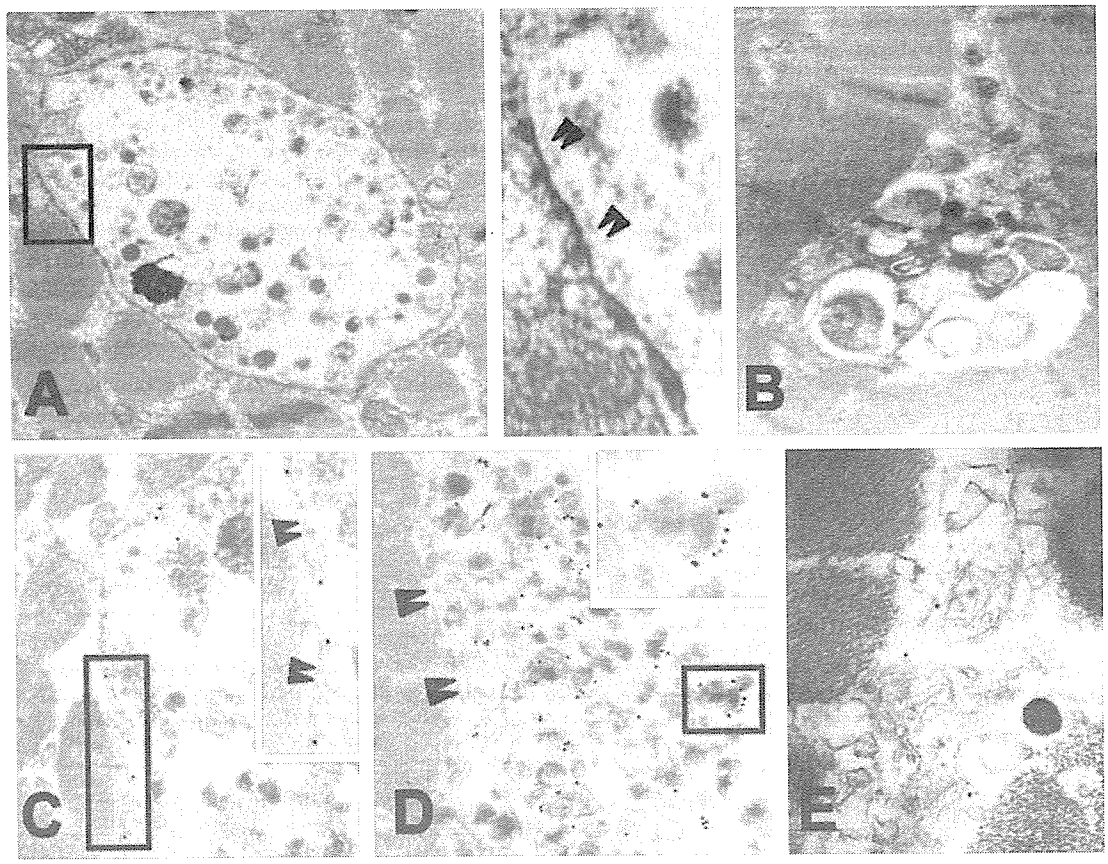

FIGURE 5. Electron micrograph in muscle from Danon disease patient. Scattered in the muscle fibers were clusters of autophagic vacuoles (A) containing cytoplasmic debris, electron dense material, and myeloid bodies. Some of these clusters were encircled by a membrane with basal lamina (paired arrowheads) on its luminal side, while other clusters are not limited by a membrane (B). Electron immunohistochemistry after single labeling with dystrophin or LIMP-1 antibody shows localization of the proteins in autophagic vacuoles (C–E). In the clusters with membranes, that is, the AVSF (A), the immunogold particles show dystrophin (C) along the vacuolar membrane (paired arrowheads), and the immunogold particles show LIMP-1 (D) around autophagic material inside autophagic vacuoles. In contrast, in the clusters not surrounded by membranes, immunogold particles show LIMP-1 around autophagic materials with absence of dystrophin (E). Original magnifications: (A) 15,000×; (B) 18,000×; (C) 20,000×; (D) 18,000×; (E) 30,000×.

unusual autophagic vacuoles with unique sarcolemmal features.

TfR and LDL-R are found in the membranes of recycling endosomes. In contrast, Rab5 and VAMP-7 are present in the membranes of early and late endosomes (29). We revealed the presence of all of these proteins in the fibers with autophagic vacuoles, indicating that in addition to the lysosomal system, the endosomal system is activated in Danon disease and related AVMs. Interestingly, VAMP-7 was increased in nonvacuolated fibers without autolysosomal accumulations, suggesting that maturation to late endosomes could prevent the formation of the unique vacuolar membranes.

Most of the vacuolar membranes were closed and were not connected to the sarcolemma in Danon disease. The autolysosomes containing cytoplasmic debris are therefore seen to be entrapped within the lumen of the vacuoles, and as such can be possibly considered to be extracellular space. Together with the observations that most AVSF did not accumulate in the subsarcolemmal region but were scattered in the cytoplasm, our findings suggest that the unique vacuolar membranes may be formed in situ in cytoplasm by a mechanism other than indentation of sarcolemma. One hypothesis is that the vacuolar membrane with basal lamina might be produced around clusters of autolysosomes (Fig. 6). The membranes surrounding the autophagic vacuoles might have originated from the lysosomal membrane or the isolation membrane that elongates and develops into the membrane of autophagosome (30), or is formed in situ and entirely de novo. If the vacuolar membranes are formed within the muscle fibers, it is compatible with the observation that the vacuolar membranes lack collagens IV and VI because collagens are thought to be produced mainly in the interstitium. Further studies are still necessary to understand the mechanism of the formation of these peculiar vacuolar membranes.

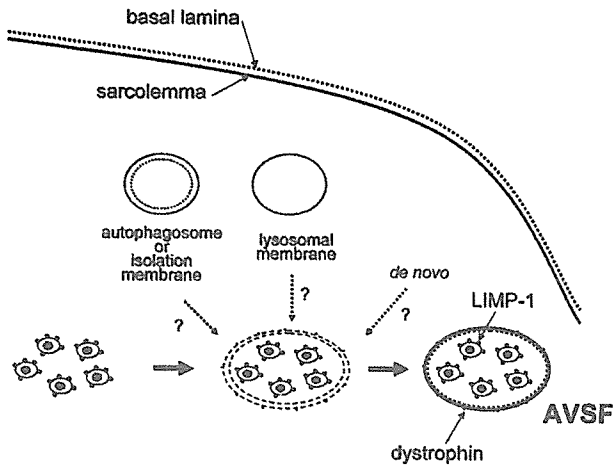

FIGURE 6. Schematic diagram of autophagic vacuoles in muscle fiber of patients with Danon disease. The membranes of the AVSFs were closed and were not connected to the sarcolemma. We suggest that the unique vacuolar membranes may be formed in situ in cytoplasm by a mechanism. One hypothesis is that the vacuolar membrane with basal lamina might be produced around clusters of autolysosomes, as illustrated.

In XMEA, vacuolar membranes have not been reported to have AChE activity (6). However, the strong similarity of the pathologic characteristics to Danon disease naturally raised the question of whether AChE activity is present in the vacuolar membranes in XMEA. Indeed, our Japanese patient with probable XMEA showed AChE activity in the vacuolar membranes. Therefore, Danon disease, XMEA, infantile AVM, and adult-onset AVM with multiorgan involvement share a common pathologic feature, namely, AVSF with AChE activity in the vacuolar membranes. Nevertheless, XMEA, infantile AVM, and adult-onset AVM are genetically different from Danon disease, as indicated by the presence of LAMP-2, which is absent in Danon disease. The observation that some features are not seen in Danon disease, like the presence of multilayered basal lamina and the deposition of C5b-9 over the surface of the muscle fiber, raise a possibility that some of these diseases might be allelic to XMEA, albeit different clinical phenotypes.

The autophagic vacuoles in AMD and rimmed vacuoles were reported to occasionally show presence of dystrophin. Nevertheless, these vacuoles are distinct from the AVSF seen in Danon disease and related AVMs, because the frequency of the vacuoles with sarcolemmal features is much less and most of sarcolemmal proteins are not consistently present in the vacuolar membranes of AMD and the rimmed vacuolar myopathies. Moreover, the activities of AChE and NSE were never found in the vacuolar membranes of these myopathies. In addition, on electron microscopy, the vacuolar membranes with basal lamina, such as those seen in Danon disease and related AVMs, were not found in AMD, DMRV/HIBM, or SIBM. According to the classification of De Bleecker et al, the AVSF may belong to type 1 vacuoles as the boundaries of type 1 vacuoles reacted for laminin, β-spectrin, and dystrophin (31). However, type 1 vacuoles were thought to be open to extracellular space and arise from invagination of the sarcolemma. Moreover, the membranes of AVSF have not only many sarcolemmal and extracellular proteins but also AChE activity, and may be formed in situ in cytoplasm as described above. Therefore, we think that the AVSF are a new, highly specific subtype of type 1 vacuoles.

Although the mechanism of their production still remains a mystery, overall, AVSF with AChE activity delineate Danon disease, XMEA, infantile AVM, and adult-onset AVM with multiorgan involvement from other AVMs. Most likely, this unique pathologic finding will probably be found in more diseases and therefore the list of AVMs in this group is likely to expand.

ACKNOWLEDGMENTS

The authors thank Drs. Shuzo M. Sumi (University of Washington, Seattle, WA) and May Christine V. Malicdan (NCNP, Tokyo, Japan) for their reviewing the manuscript. We also thank Dr. Michihiro Imamura (NCNP, Tokyo, Japan) for rabbit polyclonal anti-dystrophin antibody, Dr. Thierry Galli (Institut du Fer-à-Moulin, Paris, France) for mouse monoclonal anti-VAMP-7 antibody, Dr. Janice E. Sugiyama (National Institutes of Health, Bethesda, MD) for rabbit polyclonal anti-agrin antibody, and Dr. Yoshitaka Tanaka (Kyushu University, Fukuoka, Japan) for mouse monoclonal anti-LIMP-2 antibody. The authors thank Ms. Rika Oketa, Chiharu Yoshioka, and Fumie Uematsu (NCNP, Tokyo, Japan) for their technical assistance.

REFERENCES

1. Nishino I, Fu J, Tanji K, et al. Primary LAMP-2 deficiency causes X-linked vacuolar cardiomyopathy and myopathy (Danon disease). Nature 2000;406:906–10
2. Danon MJ, Oh SJ, DiMauro S, et al. Lysosomal glycogen storage disease with normal acid maltase. Neurology 1981;31:51–57
3. Sugie K, Yamamoto A, Murayama K, et al. The clinicopathological features of genetically confirmed Danon disease. Neurology 2002;58: 1773–78
4. Nishino I, Yamamoto A, Sugie K, Nonaka I, Hirano M. Danon disease and related disorders. Acta Myologica 2001;20:120–24
5. Murakami N, Goto Y, Itoh M, et al. Sarcolemmal indentation in cardiomyopathy with mental retardation and vacuolar myopathy. Neuromuscul Disord 1995;5:149–55
6. Kalimo H, Savontaus ML, Lang H, et al. X-linked myopathy with excessive autophagy: A new hereditary muscle disease. Ann Neurol 1988;23: 258–65
7. Yamamoto A, Morisawa Y, Verloes A, et al. Infantile autophagic vacuolar myopathy is distinct from Danon disease. Neurology 2001;57:903–5
8. Kaneda D, Sugie K, Yamamoto A, et al. A novel form of autophagic vacuolar myopathy with late-onset and multiorgan involvement. Neurology 2003;61:128–31
9. Nishino I. Autophagic vacuolar myopathies. Curr Neurol Neurosci Rep 2003;3:64–69
10. Tanaka Y, Guhde G, Suter A, et al. Accumulation of autophagic vacuoles and cardiomyopathy in LAMP-2-deficient mice. Nature 2000;406: 902–6
11. Saftig P, Tanaka Y, Lullmann-Rauch R, von Figura K. Disease model: LAMP-2 enlightens Danon disease. Trends Mol Med 2001;7:37–39
12. Sugie K, Koori T, Yamamoto A, et al. Characterization of Danon disease in a male patient and his affected mother. Neuromuscul Disord 2003;13: 708–11
13. Nishino I, Noguchi S, Murayama K, et al. Distal myopathy with rimmed vacuoles is allelic to hereditary inclusion body myopathy. Neurology 2002;59:1689–93

14. Takemitsu M, Nonaka I, Sugita H. Dystrophin-related protein in skeletal muscles in neuromuscular disorders: Immunohistochemical study. Acta Neuropathol 1993;85:256–59
15. Metzinger L, Blake DJ, Squier MV, et al. Dystrobrevin deficiency at the sarcolemma of patients with muscular dystrophy. Hum Mol Genet 1997;6:1185–91
16. Ozawa E, Nishino I, Nonaka I. Sarcolemmopathy: Muscular dystrophies with cell membrane defects. Brain Pathol 2001;11:218–30
17. Tinsley JM, Blake DJ, Roche A, et al. Primary structure of dystrophin-related protein. Nature 1992;360:591–93
18. Collo G, Starr L, Quaranta V. A new isoform of the laminin receptor integrin α7β1 is developmentally regulated in skeletal muscle. J Biol Chem 1993;268:19019–24
19. Minetti C, Sotgia F, Bruno C, et al. Mutations in the caveolin-3 gene cause autosomal dominant limb-girdle muscular dystrophy. Nat Genet 1998;18: 365–68
20. Matsuda C, Aoki M, Hayashi YK, Ho MF, Arahata K, Brown RH Jr. Dysferlin is a surface membrane-associated protein that is absent in Miyoshi myopathy. Neurology 1999;53:1119–22
21. Kuo HJ, Maslen CL, Keene DR, Glanville RW. Type VI collagen anchors endothelial basement membranes by interacting with type IV collagen. J Biol Chem 1997;272:26522–29
22. Matthews-Bellinger JA, Salpeter MM. Fine structural distribution of acetylcholine receptors at developing mouse neuromuscular junctions. J Neurosci 1983;3:644–57
23. Ishikawa Y, Shimada Y. Acetylcholine receptors and cholinesterase in developing chick skeletal muscle fibers. Brain Res 1982;281:187–97
24. Fukuda M. Biogenesis of the lysosomal membrane. Subcell Biochem 1994;22:199–230
25. Winchester BG. Lysosomal membrane proteins. Eur J Paediat Neurol 2001;5:11–19
26. Kannan K, Divers SG, Lurie AA, Chervenak R, Fukuda M, Holcombe RF. Cell surface expression of lysosome-associated membrane protein-2 (lamp2) and CD63 as markers of in vivo platelet activation in malignancy. Eur J Haematol 1995;55:145–51
27. Reddy A, Caler EV, Andrews NW. Plasma membrane repair is mediated by Ca(2+)-regulated exocytosis of lysosomes. Cell 2001;106:157–69
28. Engel AG. Acid maltase deficiency. In: Engel AG, Banqer BQ, eds. *Myology*, Vol. 2. New York, NY: McGraw-Hill, 1993:1533–53
29. Advani RJ, Yang B, Prekeris R, Lee KC, Klumperman J, Scheller RH. VAMP-7 mediates vesicular transport from endosomes to lysosomes. J Cell Biol 1999;146:765–76
30. Mizushima N, Yamamoto A, Hatano M, et al. Dissection of autophagosome formation using Apg5-deficient mouse embryonic stem cells. J Cell Biol 2001;152:657–67
31. De Bleecker JL, Engel AG, Winkelmann JC. Localization of dystrophin and β-spectrin in vacuolar myopathies. Am J Pathol 1993;143:1200–1208
32. Sugiyama JE, Glass DJ, Yancopoulos GD, Hall ZW. Laminin-induced acetylcholine receptor clustering: An alternative pathway. J Cell Biol 1997;139:181–91

THE JOURNAL OF BIOLOGICAL CHEMISTRY VOL. 281, NO. 10, pp. 6442–6447, March 10, 2006

Leukemia Inhibitory Factor Induces Endothelial Differentiation in Cardiac Stem Cells*

Received for publication, August 15, 2005, and in revised form, December 28, 2005 Published, JBC Papers in Press, December 28, 2005, DOI 10.1074/jbc.M508969200

Tomomi Mohri‡, Yasushi Fujio‡[1], Makiko Maeda‡, Takashi Ito‡, Tomohiko Iwakura‡, Yuichi Oshima‡, Yoriko Uozumi‡, Masashi Segawa§, Hiroshi Yamamoto§, Tadamitsu Kishimoto¶, and Junichi Azuma‡

From the ‡Department of Clinical Evaluation of Medicines and Therapeutics and §Department of Immunology, Graduate School of Pharmaceutical Sciences, and the ¶Laboratory of Immune Regulation, Graduate School of Frontier Bioscience, Osaka University, 1-6 Yamadaoka, Suita City, Osaka 565-0871, Japan

The importance of interleukin 6 (IL-6)-related cytokines in cardiac homeostasis has been studied extensively; however, little is known about their biological significance in cardiac stem cells. Here we describe that leukemia inhibitory factor (LIF), a member of IL-6-related cytokines, activated STAT3 and ERK1/2 in cardiac Sca-1 stem cells. LIF stimulation resulted in the induction of endothelial cell-specific genes, including VE-cadherin, *Flk-1*, and *CD31*, whereas neither smooth muscle nor cardiac muscle marker genes such as *GATA4*, *GATA6*, *Nkx-2.5*, and calponin were up-regulated. Immunocytochemical examination showed that about 25% of total cells were positively stained with anti-CD31 antibody 14 days after LIF stimulation. Immunofluorescent microscopic analyses identified the Sca-1 cells that were also positively stained with anti-von Willebrand factor antibody, indicating the differentiating process of Sca-1 cells into the endothelial cells. IL-6, which did not activate STAT3 and ERK1/2, failed to induce the differentiation of cardiac stem cells into the endothelial cells. In cardiac stem cells, the transduction with dominant negative STAT3 abrogated the LIF-induced endothelial differentiation. And the inhibition of ERK1/2 with the MEK1/2 inhibitor U0126 also prevented the differentiation of Sca-1 cells into endothelial cells. Thus, both STAT3 and ERK1/2 are required for LIF-mediated endothelial differentiation in cardiac stem cells. Collectively, it is proposed that LIF regulates the commitment of cardiac stem cells into the endothelial cell lineage, contributing to neovascularization in the process of tissue remodeling and/or regeneration.

Cardiac homeostasis is maintained by various kinds of extracellular signals through paracrine factors. Among these signals, interleukin 6 (IL-6)[2]-related cytokines have been demonstrated to play important roles in cardioprotection (1), vessel formation (2, 3), and cell-cell adhesion (4) in the heart. IL-6-related cytokines utilize glycoprotein 130 (gp130) as a common receptor. Signals through gp130 activate the signal transducer and activator of transcription (STAT) proteins and extracellular signal-regulated kinases 1/2 (ERK1/2) (5). Activated STAT proteins function as latent transcription factors and up-regulate a wide range of target genes, including *bcl-xL* (6), *VEGF* (7), metallothionein (1), *MnSOD* (manganese superoxide dismutase) (8), and *Wnt5a* (4). Recently it has been reported that cardiomyocyte-restricted ablation of the *STAT3* gene results in heart failure, accompanied by impairment of vessel growth and high sensitivity to cardiac injury (9, 10). Thus the importance of IL-6-related cytokines/gp130/STAT pathway has been established in cardiac myocytes; however, the possibility remains to be fully addressed that IL-6-related cytokines stimulate the non-myocyte population in the heart and contribute to cardiac homeostasis.

Previously it was believed that cardiac myocytes exited from the cell cycle immediately after birth and regenerated only to a lesser extent. However, recently, cardiac stem cells have been identified in the myocardium and demonstrated to differentiate into cardiomyocytes. Thus far, two kinds of cardiac stem cells, c-*kit* cells (11) and Sca-1 cells (12, 13), have been reported. It is demonstrated that c-*kit* cells differentiate into vascular smooth muscle cells and endothelial cells, as well as cardiac myocytes, whereas Sca-1 cells differentiate into osteoblasts or adipocytes. Despite the potential importance in the clinical application, the physiological signals responsible for the differentiation of the stem cells remain to be fully elucidated.

In the present study, we examined the regulatory mechanisms for the endothelial differentiation of cardiac Sca-1 cells. We then have demonstrated that leukemia inhibitory factor (LIF), an IL-6-related cytokine, promotes endothelial differentiation. Inhibition of STAT3 activity or ERK1/2 activity prevents endothelial differentiation, suggesting that both STAT3 and ERK play important roles in endothelial differentiation of cardiac stem cells. These data indicate that signals through gp130 could induce endothelial differentiation of cardiac stem cells as a potential source of endothelial cells. This study proposes a novel mechanism of gp130-mediated neovascularization.

MATERIALS AND METHODS

Preparation of Cardiac Sca-1 Cells—Sca-1 cardiac stem cells were prepared according to a previous report (13) with minor modification. Briefly, hearts from adult C57Bl/6 mice (10–12 weeks old; Japan SLC) were treated with 0.1% collagenase for 30 min (12). Cells were filtered through 80- m mesh and suspended in PBS supplemented with 3% FBS. To separate Sca-1 cells, cells were incubated with biotinylated anti-Sca-1 antibody (BD Biosciences) for 15 min on ice and washed with IMag buffer (consisting of PBS with 0.5% bovine serum albumin and 2 mM EDTA) followed by incubation with streptavidin-conjugated particles for 30 min on ice. The labeled cells were resuspended in IMag buffer, and the Sca-1 cells were separated from the cell suspension by using IMagnet (BD IMag Cell Separation System, BD Biosciences)

* This work was supported by a grant-in-aid for scientific research from the Ministry of Education, Science, Sports, and Culture of Japan and The Pharmacological Research Foundation, Tokyo. The costs of publication of this article were defrayed in part by the payment of page charges. This article must therefore be hereby marked "*advertisement*" in accordance with 18 U.S.C. Section 1734 solely to indicate this fact.

[1] To whom correspondence should be addressed: Dept. of Clinical Evaluation of Medicines and Therapeutics, 1-6 Yamadaoka, Suita City, Osaka, 565-0871, Japan. Tel.: 81-6-6879-8252; Fax: 81-6-6879-8253; E-mail: fujio@phs.osaka-u.ac.jp.

[2] The abbreviations used are: IL-6, interleukin-6; LIF, leukemia inhibitory factor; STAT, signal transducer and activator of transcription; ERK, extracellular signal-regulated kinase; Sca-1, stem cell antigen-1; gp130, glycoprotein 130; vWF, von Willebrand factor; mNSCM, modified neural stem cell medium; bFGF, basic fibroblast growth factor; EGF, epidermal growth factor; RT, reverse transcriptase; dnSTAT3, dominant negative STAT3;PBS, phosphate-buffered saline; FBS, fetal bovine serum.

according to the manufacturer's protocol. Flow cytometric analysis confirmed that the 97.6 1.1% of the cells were Sca-1 positive cells, which is consistent with previous studies (12, 13).

Newly isolated cardiac Sca-1 cells were incubated in Iscove's modified Dulbecco's medium supplemented with 10% FBS overnight. To maintain multipotency of the differentiation, Sca-1 cells were cultured in mNSCM (modified neural stem cell medium) consisting of Dulbecco's modified Eagle's medium and Ham's F12 (ratio 1:1) supplemented with 5 mM HEPES, ITS (5 g/ml insulin, 5 g/ml transferrin, and 5 ng/ml sodium selenite), 10 ng/ml bFGF, 20 ng/ml EGF, and 1000 units/ml LIF (11) as described under "Results." In some experiments, Sca-1 cells were amplified in mNSCM and used for the assay.

TABLE 1
PCR primers used in the present study

Genes	Direction	Sequence
VE-cadherin	Forward	5 -ATCTTCCTCTGCATCCTCAC-3
	Reverse	5 -GTAAGTGACCAACTGCTCGT-3
Flk-1	Forward	5 -TGCCGGCATGGTCTTCTGTGAGG-3
	Reverse	5 -CATTGAGCTCTGTTCTCGCTGTAC-3
CD31	Forward	5 -GAGCCCAATCACGTTTCAGTTT-3
	Reverse	5 -TCCTTCCTGCTTCTTGCTAGCT-3
Nkx-2.5	Forward	5 -CAGTGGAGCTGGACAAAGCC-3
	Reverse	5 -TTGTAGCGACGGTTCTGGAA-3
GATA4	Forward	5 -CTGTCATCTCACTATGGGCA-3
	Reverse	5 -CCAAGTCCGAGCAGGAATTT-3
Calponin	Forward	5 -GCACATTTTAACCGAGGTCC-3
	Reverse	5 -TGACCTTCTTCACAGAACCC-3
GATA6	Forward	5 -AAAGCTTGCTCCGGTAACAG-3
	Reverse	5 -GGACAGACTGACACCTATGT-3
GAPDH	Forward	5 -CATCACCATCTTCCAGGAGCG-3
	Reverse	5 -GAGGGGCCATCCACAGTCTTC-3

LIF was purchased from Chemicon International. IL-6, bFGF, and EGF were purchased from Peprotech EC (London, UK). U0126 (Cell signaling, MA), a highly selective inhibitor for MEK1/2, was used for the inhibition of ERK1/2.

Immunoblot Analyses—Immunoblotting was performed as described previously (14). Briefly, cells were stimulated with IL-6-related cytokines for the indicated time. After being washed with ice-cold PBS twice, cell lysates were prepared by the addition of SDS-PAGE sample buffer and boiled for 5 min. Proteins were separated by SDS-PAGE and transferred onto polyvinylidene difluoride membrane (Millipore, MA). The membrane was blocked with 2% skim milk and incubated with anti-phospho-STAT3, anti-phospho-ERK1/2, or anti-phospho-Akt (all from Cell Signaling) antibody as a first antibody. ECL system was used for detection. To quantify the extent of phosphorylation, the membranes were reprobed with anti-STAT3 (Santa Cruz Biotechnology, Santa Cruz, CA), anti-ERK1/2 (Cell Signaling), or anti-Akt (Cell Signaling) antibody. The band intensities of phospho-proteins were normalized with those of total proteins. The activities of phospho-specific antibodies were confirmed by using the extract from cardiomyocytes stimulated LIF as a positive control.

RT-PCR Analyses—RT-PCR was performed as described previously (6). Briefly, total RNA was prepared using the acid guanidinium thiocyanate-phenol-chloroform method (15). Total RNA (1 g) was subjected to first strand cDNA synthesis by using the oligo(dT) first strand primer. Gene-specific primers used for PCR amplification are shown in Table 1. The PCR products were size-fractionated by 2% agarose gel electrophoresis and detected by staining with ethidium bromide.

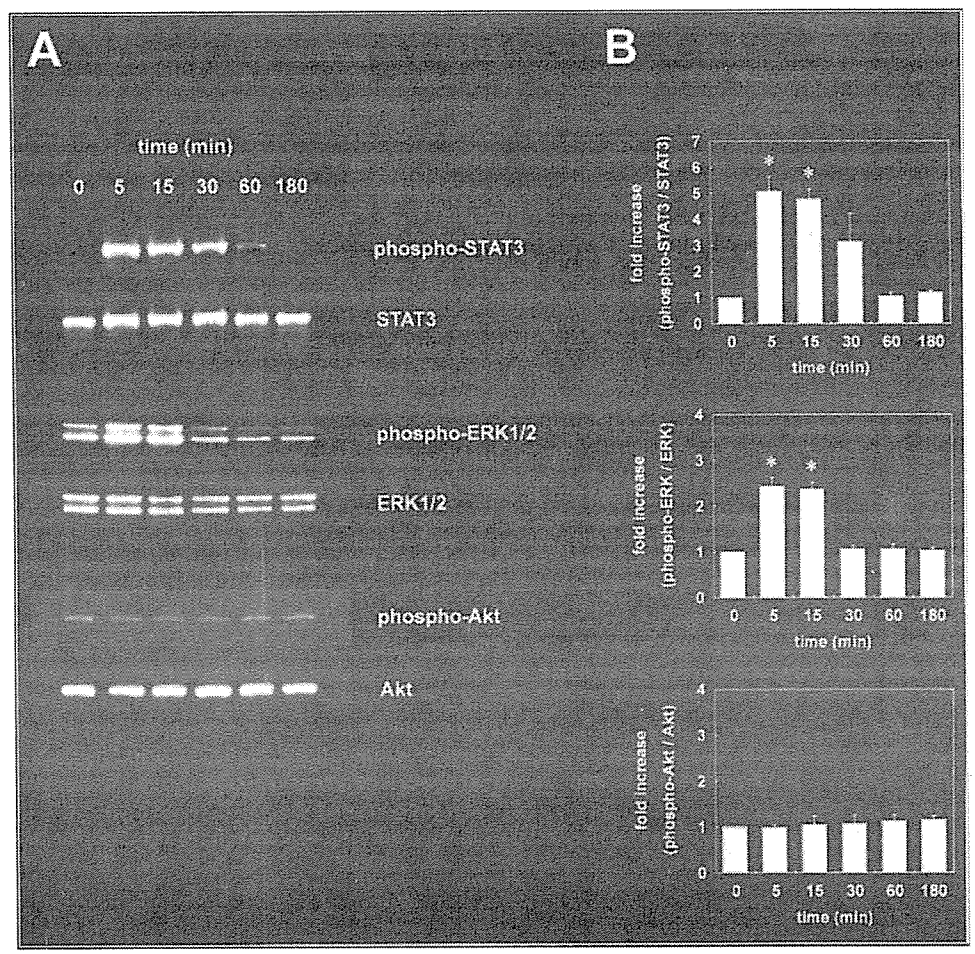

FIGURE 1. **LIF activates STAT3 and ERK, but not Akt, in cardiac Sca-1 cells.** Cardiac Sca-1 cells were stimulated by 1000 units/ml LIF for the indicated time. Cell lysates were immunoblotted with anti-phospho-STAT3, anti-phospho-ERK1/2, or anti-phospho-Akt antibody. Blots were reprobed with anti-STAT3, anti-ERK1/2, or anti-Akt antibody. *A*, representative data are shown. *B*, quantitative analysis of tyrosine phosphorylation of STAT3, ERK1/2, and Akt. The band intensities of phospho-proteins were normalized with that of total proteins. Data are presented as means S.E. (n 3). *, p 0.05 *versus* control (paired t test).

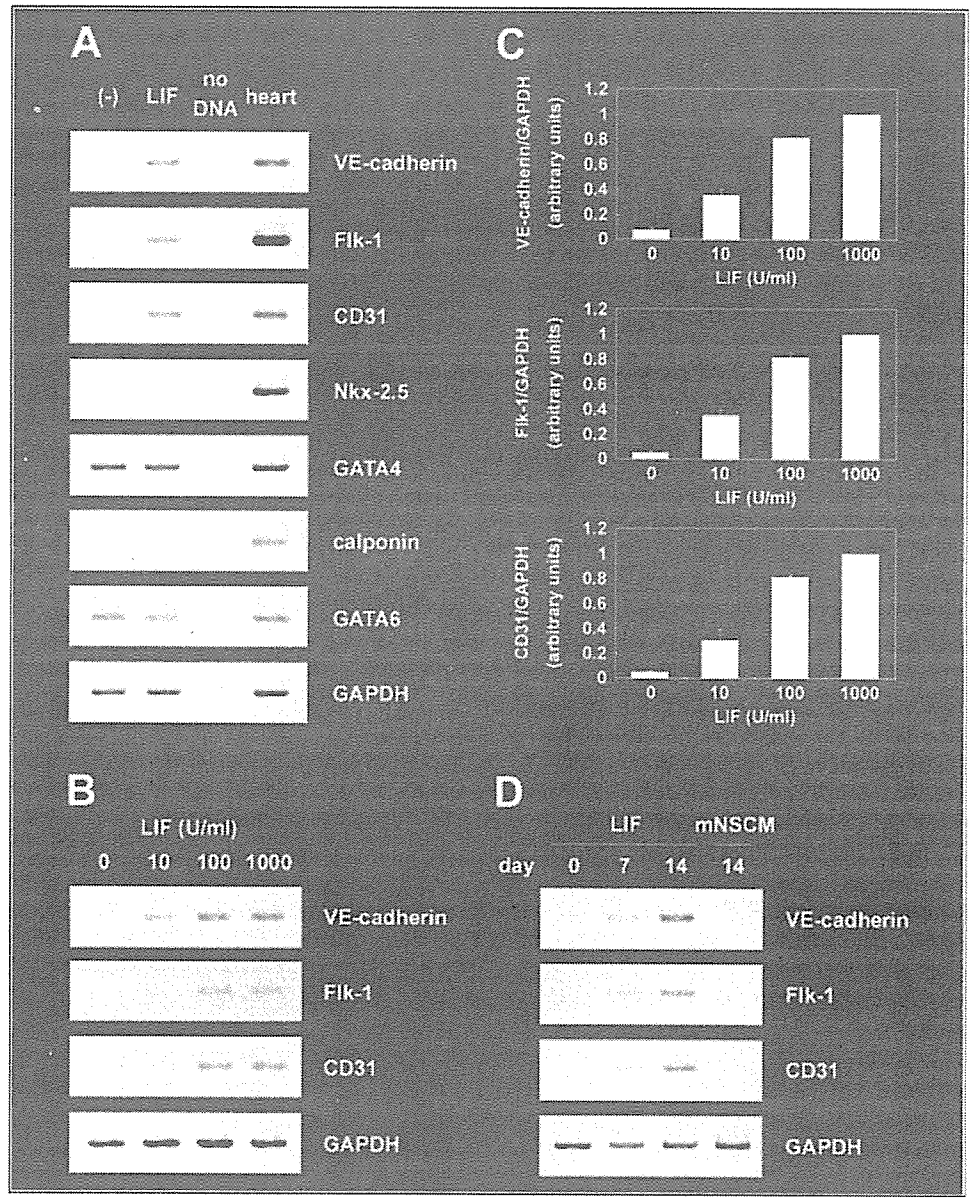

FIGURE 2. **Signals through gp130 up-regulate endothelial cell-specific marker genes in cardiac Sca-1 cells.** *A*, cardiac Sca-1 cells were stimulated with or without LIF (1000 units/ml) for 14 days. Total RNA was prepared, and RT-PCR was performed for as described under "Materials and Methods." Total RNA prepared from heart was used as positive control. GAPDH was used as an internal control. Experiments were repeated three times with similar results. *B* and *C*, Sca-1 cells were cultured with the indicated concentrations of LIF for 14 days. Total RNA was prepared, and RT-PCR was performed for the endothelial cell-specific genes. GAPDH was used as an internal control. Experiments were repeated three times with similar results. Representative data are shown in *B*. The band intensities of endothelial markers were normalized with that of GAPDH. Data are presented as means S.E. (*n* 3) (*C*). *D*, Sca-1 cells were maintained in mNSCM containing EGF, bFGF, and LIF for 10 days followed by cultivation in medium containing only LIF (1000 units/ml) or in mNSCM for the indicated time. Total RNA was prepared, and RT-PCR was performed. GAPDH was used as an internal control. Experiments were repeated three times with similar results.

Immunocytochemical Examination—Cells were fixed with 3.7% formaldehyde in PBS for 20 min at room temperature and incubated with anti-CD31 antibody (BD Biosciences) followed by the incubation with alkaline phosphatase-conjugated secondary antibody (Santa Cruz Biotechnology). Cells were washed with Tris-buffered saline and incubated in 5-bromo-4-chloro-3-indolyl phosphate/nitro blue tetrazolium solution (BCIP/NBT, Sigma). After staining, positively stained cells were counted by a person who was blinded to the culture conditions.

Immunofluorescent Examination—Immunofluorescent microscopic analyses were performed as described previously (16). Briefly, cells were fixed with 3.7% formaldehyde in PBS for 20 min at room temperature and stained with anti-Sca-1 (R&D Systems) and anti-von Willebrand factor antibodies (Santa Cruz Biotechnology). Alexa Fluor 488- or 546-conjugated secondary antibody (Molecular Probes) was used for detection. Nuclei were stained with Hoechst dye. Cells were examined by Olympus IX70.

Adenovirus Vectors—Generation of the adenovirus vector expressing dominant negative STAT3 (dnSTAT3) was described previously (17). Adenovirus vector expressing -galactosidase was used as a control.

Adenovirus vectors were amplified in HEK293 cells and purified by CsCl ultracentrifugation (18). Sca-1 cells were infected at a multiplicity of infection of 100 for 12 h and cultured under the indicated conditions. By this method, more than 90% of Sca-1 cells were transfected with adenovirus vectors (data not shown).

Statistical Analysis—Statistical significance was determined by paired *t* test or Student's *t* test. Data were presented as mean S.E., and p 0.05 was considered statistically significant.

RESULTS

LIF Activates STAT3 and ERK1/2 in Cardiac Stem Cells—Signals through gp130 play important roles in cardiac homeostasis. Recently, cardiac stem cells have been reported to contribute to cardiac repair and regeneration (11, 12). Thus, we examined whether signals through gp130 are transduced in cardiac stem cells. Cardiac Sca-1 cells were stimulated with LIF for the indicated time. Cell lysates were prepared, and activation of STAT3, ERK1/2, and Akt was analyzed by immunoblotting with phospho-specific antibodies (Fig. 1*A*). STAT3 and ERKs,

but not Akt, were phosphorylated by LIF stimulation. STAT3 and ERKs were activated within 5 min of LIF stimulation (Fig. 1*B*).

LIF Induces Endothelial Differentiation in Cardiac Stem Cells—We examined the effects of LIF on the differentiation of Sca-1 cells. By RT-PCR (Fig. 2*A*), it was revealed that LIF induced VE-cadherin, *Flk-1*, and *CD31*, marker genes for endothelial cells, whereas *Nkx-2.5* and calponin was not up-regulated by LIF. GATA4 and GATA6 were expressed in nonstimulated Sca-1 cells, and their expression was not affected by LIF. LIF induced the expression of endothelial marker genes in a dose-dependent manner (Fig. 2, *B* and *C*). The endothelial markers were submaximally induced by 100units/ml LIF.

Previously it was reported that cardiac c-*kit* stem cells could be maintained as undifferentiated cells in mNSCM, Dulbecco's modified Eagle's medium, and Ham's F12 (ratio 1:1) containing bFGF, EGF, and LIF (11). Thus we analyzed the expression of the endothelial markers in Sca-1 cells cultured in mNSCM. In mNSCM, cardiac Sca-1 cell population did not express endothelial marker genes; however, cells were differentiated into endothelial cells when moved to the medium containing only LIF (Fig. 2*D*). The induction of endothelial marker genes was detected 7 days after stimulation, and afterward their expression increased. These data suggest that Sca-1 cells can be maintained in the presence of bFGF, EGF, and LIF without impairing the potential for endothelial differentiation. In preliminary studies, we noticed that cardiac Sca-1 cells occasionally showed expression of CD31, an endothelial marker, as described previously (12), when cultured in the presence of FBS more than 5 days and that FBS-mediated differentiation depended on the batches of FBS (data not shown). Therefore, in the present study, Sca-1 cells were amplified in mNSCM. Sca-1 cells cultured in mNSCM without LIF showed reduced potential for differentiation into endothelial cells, suggesting that LIF could contribute to maintenance of the potential for endothelial differentiation from Sca-1 cells in the presence of bFGF and EGF (data not shown).

To estimate the frequency of endothelial differentiation from Sca-1 cell culture, cells were cultured in the presence or absence of LIF for the indicated time and stained with anti-CD31 antibody (Fig. 3*A*). At day 3, CD31 cells were not observed either in the presence or absence of LIF. Cells positively stained with anti-CD31 antibody were detected 7 days after LIF stimulation. Thereafter, the frequency of CD31 cells increased up to about 25% of total cells 14 days after LIF stimulation (Fig. 3*B*). In contrast, CD31 cells were not significantly detected when the cells were cultured in the absence of LIF. We analyzed the effects of bFGF on LIF-induced endothelial differentiation because bFGF is also known to be a potent angiogenic growth factor, and it was found that co-stimulation with bFGF and LIF did not increase the number of CD31 positive cells, as compared with LIF stimulation (data not shown).

The cardiac stem cells were cultured in the presence of LIF for 14 days and co-stained with anti-Sca-1 and anti-von Willebrand factor (vWF) antibodies (Fig. 4). Immunofluorescent microscopic analyses detected Sca-1 cells that also showed positive staining for vWF, an endothelial marker, thus suggesting the transition from Sca-1 cells to endothelial lineage.

Both STAT3 and ERK1/2 Are Required for LIF-mediated Endothelial Differentiation—To analyze the signaling pathways involved in endothelial differentiation, we tested the effects of IL-6, which utilizes gp130 as one subunit of its receptor system. In contrast to LIF, IL-6 did not activate STAT3 or ERK1/2 in cardiac stem cells (Fig. 5*A*). Consistently, the endothelial cell-specific genes, including VE-cadherin, *Flk-1*, and *CD31*, were not increased in response to IL-6 (Fig. 5*B*). We also addressed the additional effects of IL-6 to LIF-mediated endothelial differentiation; however, endothelial differentiation, induced by LIF, was not enhanced by co-stimulation with IL-6 (Fig. 5*C*). Thus, further efforts were made to address the functional significance of STAT3 and ERK1/2.

To examine whether STAT3 activity is involved in the endothelial differentiation of Sca-1 cells by LIF, we analyzed the effects of the inhibition of STAT3 by using adenovirus vectors expressing dnSTAT3 (Fig. 6*A*). LIF failed to induce the endothelial markers in dnSTAT3-expressing cells, whereas endothelial marker genes were up-regulated in

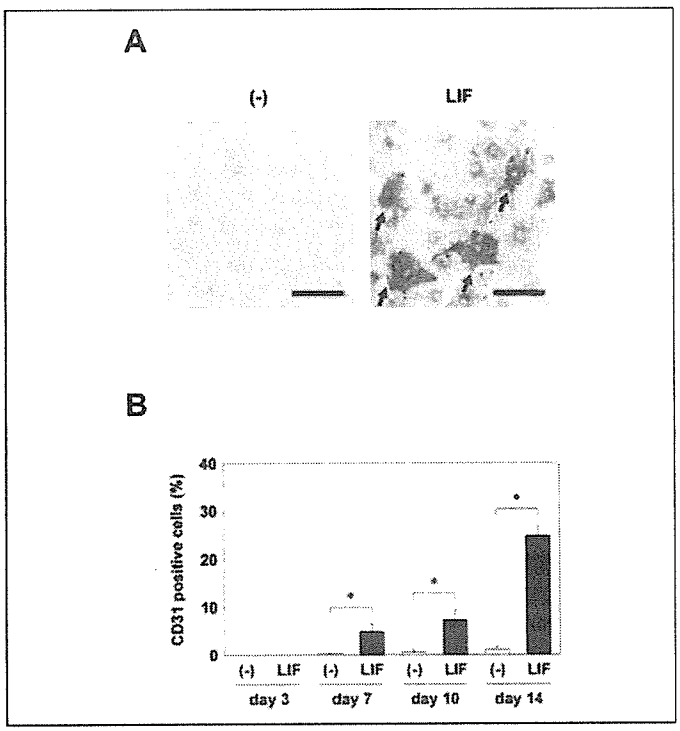

FIGURE 3. **Quantitative estimation of the frequency of the differentiation of Sca-1 cells into endothelial cells.** Cardiac Sca-1 cells were cultured in medium containing 0 or 1000 units/ml LIF for the indicated time and then stained with anti-CD31 antibody. *A*, cells were cultured in the presence or absence of LIF for 14 days. Representative immunocytochemical microscopic images were shown (magnification 100, *scale bar* 100 m). *Arrows* indicate CD31-positive cells. *B*, cells were cultured in the presence or absence of LIF for the indicated time. Cells were stained with anti-CD31 antibody. The frequency of CD31-positive cells was calculated in five fields. Each field contains 80–100 cells. Data are shown as mean S.E. *, p 0.05 (Student's t test). Experiments were repeated three times with similar results.

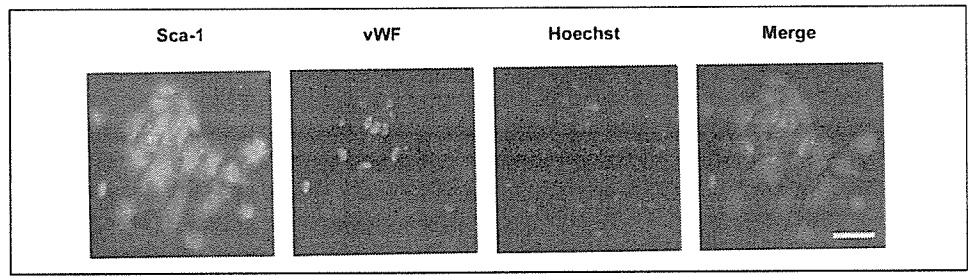

FIGURE 4. **LIF induces the expression of vWF, an endothelial marker, in cardiac Sca-1 cells.** Cardiac Sca-1 cells were cultured in the medium containing LIF (1000 units/ml) for 14 days and co-stained with anti-Sca-1 and anti-vWF antibodies. Representative immunofluorescent microscopy was shown (magnification 100, *scale bar* 100 m). Sca-1 /vWF cells were observed in three independent cultures.

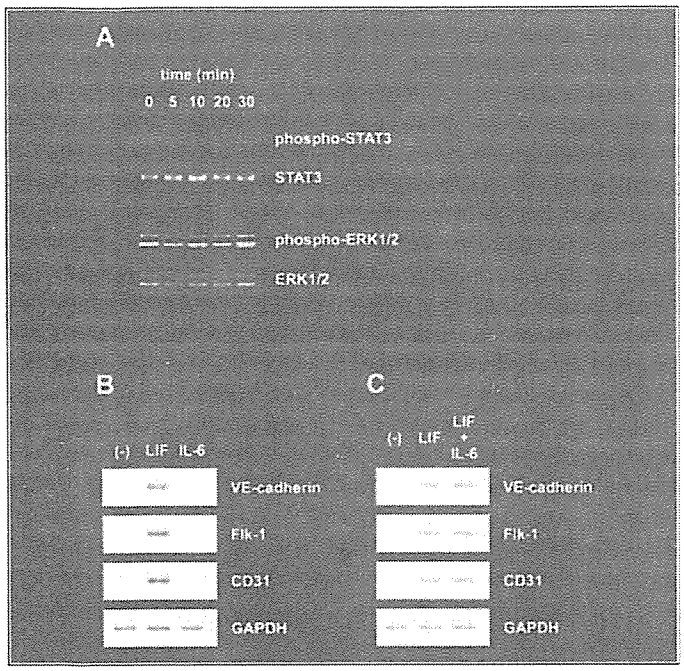

FIGURE 5. **IL-6 does not induce the expression of endothelial marker genes in cardiac Sca-1 cells.** *A*, cardiac Sca-1 cells were stimulated by IL-6 (20 ng/ml) for the indicated time. Cell lysates were prepared and immunoblotted with anti-phospho-STAT3 or anti-phospho-ERK1/2 antibody. Blots were reprobed with anti-STAT3 or anti-ERK1/2 antibody. Experiments were repeated three times with similar results. *B*, cardiac Sca-1 cells were cultured in the presence of IL-6 (20 ng/ml) or LIF (1000 units/ml) for 14 days. Total RNA was prepared, and RT-PCR was performed for endothelial cell-specific genes. GAPDH was used as an internal control. Experiments were repeated three times with similar results. *C*, to examine the additional effects of IL-6 on LIF-mediated differentiation, Sca-1 cells were cultured in the presence of LIF or LIF plus IL-6 for 14 days. Total RNA was prepared, and RT-PCR was performed for endothelial cell-specific genes. GAPDH was used as an internal control. Experiments were repeated three times with similar results.

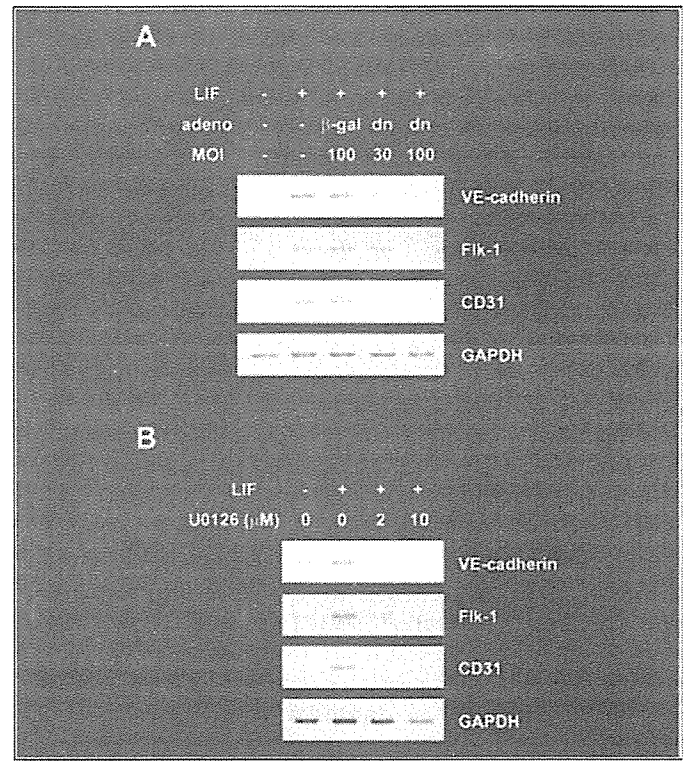

FIGURE 6. **LIF induces endothelial differentiation of cardiac Sca-1 cells through STAT3 and ERK1/2.** *A*, cardiac Sca-1 cells were transduced with adenovirus vectors (*adeno*) expressing dominant negative STAT3 (*dn*) or -galactosidase (*-gal*) as a control at the indicated multiplicity of infection (*MOI*) and cultured with ( ) or without ( ) LIF (100 units/ml) for 14 days. Total RNA was prepared, and expression of endothelial marker genes was examined by RT-PCR. GAPDH was used as an internal control. Experiments were repeated three times with similar results. *B*, cardiac Sca-1 cells were cultured in the presence or absence of LIF (100 units/ml) with or without U0126, an ERK inhibitor. Total RNA was prepared, and expression of endothelial marker genes was examined by RT-PCR. GAPDH was used as an internal control. Experiments were repeated three times with similar results.

the cells adenovirally transfected with -galactosidase, a control. Next, we tested the effects of U0126, an MEK inhibitor, on the endothelial differentiation of cardiac stem cells (Fig. 6*B*). The inhibition of ERK1/2 with U0126 inhibited the induction of endothelial marker genes by LIF. These data indicate that both STAT3 activity and ERK activity are required for the LIF-mediated differentiation of Sca-1 cells into endothelial cells. We confirmed that neither transfection of dnSTAT3 nor treatment with U0126 increased the frequency of pyknotic nuclei as analyzed by Hoechst staining, suggesting that neither inhibition of STAT3 nor of ERK affected cell viability (data not shown).

DISCUSSION

In the present study, we have demonstrated that LIF induced endothelial differentiation in cardiac stem cells. LIF stimulation rapidly activated STAT3 and ERK1/2 in cardiac stem cells. LIF up-regulated endothelial cell-specific genes without inducing either smooth muscle- or cardiac muscle-specific markers. The inhibition of STAT3 or ERK pathways abrogated endothelial differentiation, indicating that both STAT3 and ERKs are required for LIF-induced endothelial differentiation.

Initially, it was believed that postnatal neovascularization results exclusively from fully differentiated endothelial cells. However, recent studies have established that bone marrow-derived endothelial progenitor cells contribute to vessel formation (19). Endothelial progenitor cells circulate in the peripheral blood, home to the target organs, and differentiate into endothelial cells (20). In the progenitor cells, VE-cadherin and Flk-1 are highly expressed, like fully differentiated endothelial cells. In contrast, by RT-PCR we have demonstrated that neither VE-cadherin nor *Flk-1* is expressed in cardiac undifferentiated Sca-1 cells, as reported previously (12, 13). Thus, cardiac Sca-1 cells, used in the present study, are a population that is distinct from endothelial progenitors. Therefore it could be proposed that the cardiac Sca-1 population is a novel source of endothelial cells in the heart. This proposal is supported by the recent findings that skeletal muscle-derived Sca-1 cells are also differentiated into endothelial cells (21), suggesting the possible involvement of tissue-resident stem cells in vessel formation.

Cardiac Sca-1 cells are known to be differentiated into cardiomyocytes (12, 13). In the present study, we examined whether LIF induced cardiac differentiation. However, it was revealed that LIF stimulation up-regulated endothelial cell-specific genes without inducing smooth muscle or cardiomyocyte markers. In the process of *in vivo* neovascularization, differentiated endothelial cells migrate and form the capillary tubes. Therefore, we analyzed the migratory activities of LIF in cardiac Sca-1 cells; however, we could not detect an LIF-mediated increase in cell motility (data not shown). Other factors might promote the cell motility, resulting in capillary tube formation *in vivo*. LIF-induced endothelial differentiation is reminiscent of the abnormality in the placenta of LIF receptor-null mice; LIF receptor-null mice exhibit a reduction of the fetal blood vessel component in the placenta (22). It would be interesting to examine whether the tissue-resident stem cells from the peripheral organs, especially from the placenta, can be differentiated into endothelial cells by signals through gp130.

Activation of gp130 results in the rapid induction of the target genes via STAT and ERK proteins after stimulation with IL-6-related cytokines (23). Consistently, LIF rapidly activated STAT and ERK, whereas

the up-regulation of endothelial cell-specific genes such as VE-cadherin, *Flk-1*, and *CD31* was detected more than 24 h after LIF stimulation. Therefore it is unlikely that these endothelial cell-specific genes are direct targets of gp130-mediated transcriptional proteins, including STAT proteins. We examined the effects of LIF on the expression of *HoxA9* gene as an early-stage endothelial marker (24), because HoxA9 is rapidly induced by angiogenic stimuli such as shear stress and plays important roles in the expression of the endothelial genes in endothelial progenitor cells (25). However, HoxA9 was not up-regulated immediately after LIF stimulation (data not shown). Thus it is suggested that cardiac stem cells are differentiated into endothelial cells by LIF through differential mechanisms from the endothelial progenitor cells. Further studies will be required to elucidate the direct target genes of the signals through gp130 in cardiac stem cells.

The Gp130/STAT signaling pathway is activated under pathophysiological conditions in cardiac myocytes. IL-6-related cytokines are produced in cultured cardiomyocytes exposed to pathological stresses such as catecholamine, (26), mechanical stretch (27), and hypoxia (28), leading to activation of the gp130/STAT3 pathway in the myocardium. *In vivo* studies also demonstrated that LIF is up-regulated in pathological hearts, including hypertrophied hearts (29) and failing hearts (30). Moreover, LIF is produced in atrial and ventricular myocytes in failing hearts (31), suggesting the importance of the paracrine system of IL-6-related cytokines. Previously we demonstrated that activation of STAT3 promotes vessel formation through paracrine of angiogenic factors in the heart (2, 7), proposing a cardioprotective machinery via cardiomyocyte-endothelial cell interaction. Consistently, accumulating evidence has confirmed the importance of STAT3 in controlling the paracrine circuits, resulting in neovascularization in pathophysiological situations such as tumor growth (32, 33), psoriasis (34), and diabetic retinopathy (35). Here, in addition to the promotion of vessel growth through paracrine system, we propose that LIF-mediated activation of gp130 directly induces the endothelial differentiation of tissue-resident stem cells, suggesting a novel role of gp130 signaling in angiogenesis. These combined angiogenic properties may explain the prominent neovascularization induced by signals through gp130 during myocardial remodeling (3), although further efforts should be made to elucidate how much cardiac stem cells contribute to angiogenesis *in vivo*.

In summary, the present study has revealed that signals through gp130 transduce endothelial differentiation in cardiac stem cells and that IL-6-related cytokines are the paracrine factors determining the commitment of cardiac stem cells into the endothelial cell lineage. These findings propose a novel mechanism by which signals through gp130 contribute to neovascularization in the process of tissue remodeling and/or regeneration.

Acknowledgment—We thank Yasuko Murao for excellent secretarial work.

REFERENCES

1. Oshima, Y., Fujio, Y., Nakanishi, T., Itoh, N., Yamamoto, Y., Negoro, S., Tanaka, K., Kishimoto, T., Kawase, I., and Azuma, J. (2005) *Cardiovasc. Res.* **65,** 428–435
2. Osugi, T., Oshima, Y., Fujio, Y., Funamoto, M., Yamashita, A., Negoro, S., Kunisada, K., Izumi, M., Nakaoka, Y., Hirota, H., Okabe, M., Yamauchi-Takihara, K., Kawase, I., and Kishimoto, T. (2002) *J. Biol. Chem.* **277,** 6676–6681
3. Zou, Y., Takano, H., Mizukami, M., Akazawa, H., Qin, Y., Tako, H., Sakamoto, M., Minamino, T., Nagai, T., and Komuro, I. (2003) *Circulation* **108,** 748–753
4. Fujio, Y., Matsuda, T., Oshima, Y., Maeda, M., Mohri, T., Ito, T., Takatani, T., Hirata, M., Nakaoka, Y., Kimura, R., Kishimoto, T., and Azuma, J. (2004) *FEBS letters* **573,** 202–206
5. Kunisada, K., Hirota, H., Fujio, Y., Matsui, H., Tani, K., Yamauchi-Takihara, K., and Kishimoto, T. (1996) *Circulation* **94,** 2626–2632
6. Fujio, Y., Kunisada, K., Hirota, H., Yamauchi-Takihara, K., and Kishimoto, T. (1997) *J. Clin. Investig.* **99,** 2898–2905
7. Funamoto, M., Fujio, Y., Kunisada, K., Negoro, S., Tone, E., Osugi, T., Hirota, H., Izumi, M., Yoshizaki, K., Walsh, K., Kishimoto, T., and Yamauchi-Takihara, K. (2000) *J. Biol. Chem.* **275,** 10561–10566
8. Negoro, S., Kunisada, K., Fujio, Y., Darville, M. I., Eizirik, D. L., Funamoto, M., Osugi, T., Izumi, M., Oshima, Y., Nakaoka, Y., Hirota, H., Kishimoto, T., and Yamauchi-Takihara, K. (2001) *Circulation* **104,** 979–981
9. Jacoby, J. J., Kalinowski, A., Liu, M.-G., Zhang, S. S.-M., Gao, Q., Chai, G.-X., Ji, L., Iwamoto, Y., Li, E., Schneider, M., Russell, K. S., and Fu, X.-Y. (2003) *Proc. Natl. Acad. Sci. U. S. A.* **100,** 12929–12934
10. Hilfiker-Kleiner, D., Hilfiker, A., Fuchs, M., Kaminski, K., Schaefer, A., Schieffer, B., Hillmer, A., Schmiedl, A., Ding, Z., Podewski, E., Podewski, E., Poli, V., Schneider, M. D., Schulz, R., Park, J.-K., Wollert, K. C., and Drexler, H. (2004) *Circ. Res.* **95,** 187–195
11. Beltrami, A. P., Barlucchi, L., Torella, D., Baker, M., Limana, F., Chimenti, S., Kasahara, H., Rota, M., Musso, E., Urbanek, K., Leri, A., Kajstura, J., Nadal-Ginard, B., and Anversa, P. (2003) *Cell* **114,** 763–776
12. Oh, H., Bradfute, S. B., Gallardo, T., Nakamura, T., Gaussin, V., Mishina, Y., Pocius, J., Michael, L. H., Behringer, R. R., Garry, D. J., Entman, M. L., and Schneider, M. D. (2003) *Proc. Natl. Acad. Sci. U. S. A.* **100,** 12313–12318
13. Matsuura, K., Nagai, T., Nishigaki, N., Oyama, T., Nishi, J., Wada, H., Sano, M., Toko, H., Akazawa, H., Sato, T., Nakaya, H., Kasanuki, H., and Komuro, I. (2004) *J. Biol. Chem.* **279,** 11384–11391
14. Fujio, Y., and Walsh, K. (1999) *J. Biol. Chem.* **274,** 16349–16354
15. Chomczynski, P., and Sacchi, N. (1987) *Anal. Biochem.* **162,** 156–159
16. Fujio, Y., Nguyen, T., Wencker, D., Kitsis, R. N., and Walsh, K. (2000) *Circulation* **101,** 660–667
17. Kunisada, K., Tone, E., Fujio, Y., Matsui, H., Yamauchi-Takihara, K., and Kishimoto, T. (1998) *Circulation* **98,** 346–352
18. Becker, T. C., Noel, R. J., Coats, W. S., Gomez-Foix, A. M., Alam, T., Gerard, R. D., and Newgard, C. B. (1994) in *Methods in Cell Biology*, Vol. 43, pp. 161–189, Academic Press, New York
19. Asahara, T., Murohara, T., Sullivan, A., Silver, M., Zee, R., Li, T., Witzenbichler, B., Schatteman, G., and Isner, J. M. (1997) *Science* **275,** 964–967
20. Kalka, C., Masuda, H., Takahashi, T., Gordon, R., Tepper, O., Gravereaux, E., Pieczek, A., Iwaguro, H., Hayashi, S., Isner, J. M., and Asahara, T. (2000) *Circ. Res.* **86,** 1198–1202
21. Tamaki, T., Akatsuka, A., Ando, K., Nakamura, Y., Matsuzawa, H., Hotta, T., Roy, R. R., and Edgerton, V. R. (2002) *J. Cell Biol.* **157,** 571–577
22. Ware, C. B., Horowitz, M. C., Renshaw, B. R., Hunt, J. S., Liggitt, D., Koblar, S. A., Gliniak, B. C., McKenna, H. J., Papayannopoulou, T., Thoma, B., Cheng, L., Donovan, P. J., Peschon, J. J., Bartlett, P. F., Willis, C. R., Wright, B. D., Carpenter, M. K., Davison, B. L., and Gearing, D. P. (1995) *Development (Camb.)* **121,** 1283–1299
23. Kishimoto, T., Taga, T., and Akira, S. (1994) *Cell* **76,** 253–262
24. Gorski, D. H., and Walsh, K. (2000) *Circ. Res.* **87,** 865–872
25. Rossig, L., Urbich, C., Bruhl, T., Dernbach, E., Heeschen, C., Chavakis, E., Sasaki, K., Aicher, D., Diehl, F., Seeger, F., Potente, M., Aicher, A., Zanetta, L., Dejana, E., Zeiher, A. M., and Dimmeler, S. (2005) *J. Exp. Med.* **201,** 1825–1835
26. Funamoto, M., Hishinuma, S., Fujio, Y., Matsuda, Y., Kunisada, K., Oh, H., Negoro, S., Tone, E., Kishimoto, T., and Yamauchi-Takihara, K. (2000) *J. Mol. Cell. Cardiol.* **32,** 1275–1284
27. Pan, J., Fukuda, K., Saito, M., Matsuzaki, J., Kodama, H., Sano, M., Takahashi, T., Kato, T., and Ogawa, S. (1999) *Circ. Res.* **84,** 1127–1136
28. Hishinuma, S., Funamoto, M., Fujio, Y., Kunisada, K., and Yamauchi-Takihara, K. (1999) *Biochem. Biophys. Res. Commun.* **264,** 436–440
29. Kurdi, M., Randon, J., Cerutti, C., and Bricca, G. (2005) *Mol. Cell. Biochem.* **269,** 95–101
30. Podewski, E. K., Hilfiker-Kleiner, D., Hilfiker, A., Morawietz, H., Lichtenberg, A., Wollert, K. C., and Drexler, H. (2003) *Circulation* **107,** 798–802
31. Jougasaki, M., Leskinen, H., Larsen, A. M., Cataliotti, A., Chen, H. H., and Burnett, J. C. J. (2003) *Eur. J. Heart. Fail.* **5,** 137–145
32. Niu, G., Wright, K. L., Huang, M., Song, L., Haura, E., Turkson, J., Zhang, S., Wang, T., Sinibaldi, D., Coppola, D., Heller, R., Ellis, L. M., Karras, J., Bromberg, J., Pardoll, D., Jove, R., and Yu, H. (2002) *Oncogene* **21,** 2000–2008
33. Bromberg, J. (2002) *J. Clin. Investig.* **109,** 1139–1142
34. Sano, S., Chan, K. S., Carbajal, S., Clifford, J., Peavey, M., Kiguchi, K., Itami, S., and Nickoloff, B. J. (2005) *Nat. Med.* **11,** 43–49
35. Suganami, E., Takagi, H., Ohashi, H., Suzuma, K., Suzuma, I., Oh, H., Watanabe, D., Ojima, T., Suganami, T., Fujio, Y., Nakao, K., Ogawa, Y., and Yoshimura, N. (2004) *Diabetes* **53,** 2443–2448